DETECTION OF OLD AGRICULTURAL TERRACES IN STEEP, VEGETATED TERRAIN USING AIRBORNE LIDAR: CASE STUDIES FROM HONG KONG

Robert J. SAS, Jr.

Senior Geologist, Fugro (Hong Kong) Limited,

Guardian House, 7/F 32 Oi Kwan Road, Wanchai, Hong Kong;
TEL: +(852) 2577 9023;
Email: bsas@fugro.com.hk

Jason Peng YU
GIS Engineer, Fugro (Hong Kong) Limited

Carol Y.Y. PAU
Assistant Geologist, Fugro (Hong Kong) Limited

Kevin A. STYLES
Associate Director, Fugro (Hong Kong) Limited

KEY WORDS: Airborne LiDAR; Topographic Position Index (TPI); Old Terraces; Hong Kong

ABSTRACT: Old agricultural terraces and associated features are common on steep hillsides throughout the Hong Kong Special Administrative Region (HKSAR) and, since the late 1960s, most have been obscured by dense vegetation. Some of these terraces may date from a thousand or more years ago and some are still actively cultivated today. Based on aerial photograph interpretation (API) of older aerial photographs, particularly from 1963, and more recent field observations, generally these features can be classified as earthen step-form terraces, rubble wall terraces, and other forms of anthropogenic activity (e.g., military, prospecting/mining, quarrying, and *ad hoc* cuts/spoil). Their influence on slope stability is not yet well understood, however they need to be identified so that any relationship with landslide susceptibility can be better understood. Currently, these unknowns remain a potential source of residual risk for landslide hazards.

With the aim of continuous improvement of natural terrain hazard assessments, suitable detection and mapping of the terraces and other features should first be systematically undertaken. A dense tropical vegetative canopy presents an obstacle to terrace detection. Much of the HKSAR has undergone revegetation due to changing land uses, government regulations, reforestation, and rapid natural growth over the last 30 – 40 years. Many terraces and other features are visible in 1963 aerial photographs, when hillsides were relatively bare of vegetation. Additionally, many of the oldest features are degraded and, when combined with the modern, dense vegetation, may be confused with natural landscape-forming processes when observed in the field.

To assist in identification, a topographic position index (TPI) was applied to digital elevation models (DEM) derived from airborne LiDAR for three case studies. The result is an emerging, indirect mapping approach complemented by integrated API and field work to detect and map old terraces.

INTRODUCTION

Old agricultural terraces and associated features have been known to exist throughout Hong Kong for some time and were documented by early observers during the colonial past (Heanley, 1935). Ng et al. (2003), a key government document for studying landslide susceptibility in Hong Kong, describe a range of common anthropogenic disturbance including “overgrown, abandoned agricultural terraces with small masonry walls at the front.” However, most documentation only mentions old terraces and description of the widespread extent and range of the implications on slope stability of such landscape features are quite a recent occurrence (Styles & Law, 2012). The Hong Kong Government has made great efforts to reduce risk and stabilise adverse slopes using the

Landslip Prevention and Mitigation Programme (LPMitP). The slope registration programme began to document man-made slopes in the late 1970s (cut slopes, fill slopes, and retaining walls), and some more-recent old terraces have been included as registered "Disturbed Terrain," arising from work by the Geotechnical Engineering Office (GEO) in the mid-1990s. "Disturbed Terrain" is a slope classification that essentially is used to record hillsides steeper than 15° containing a "series of composite cut and/or fill slopes" (GEO, 2004). Most of the Disturbed Terrain features are marginal to areas of existing development, having been identified in areas of old hillside squatter villages which were mostly cleared in the mid-late 1980's, such as those in Shau Kei Wan, northeast Hong Kong Island.

Recent observations indicate that some old agricultural terraces are associated with landslides (**Figure 1a**). These landslides are triggered by rainfall and occur as shallow translational failures, rotational slumps, debris avalanches, debris slides, and may subsequently channelise as debris flows. The relationship between landslides, slope stability, and such anthropogenic features is not yet clear. Recent observations of some landslide features indicate that old terraces can aid in debris retention, tend to flatten slope profiles, and reduce the run-out velocity during debris flow. Numerous examples exist of terrace features across drainage lines that have not been entrained when subjected to debris flow, and therefore, are either benign or possibly beneficial to slope stability (**Figure 1b**). Landslides can occur where head scarps are aligned along contour with terraces or aligned with lateral margins along slope associated with man-made drainage features. "Tension crack-like" features have been observed in areas of pervasive old terraces and may be either indicative of shallow local failure of the terrace, soil creep, incipient regolith failure associated with the step-like form of displacement associated with a "tension crack", or more simply a case of morphological features associated with the antecedent land use. However, interpretations of these observations are difficult due to dense vegetation and the occurrence of relict geological structures in the shallow subsurface of deeply-weathered rock and weathered colluvium.

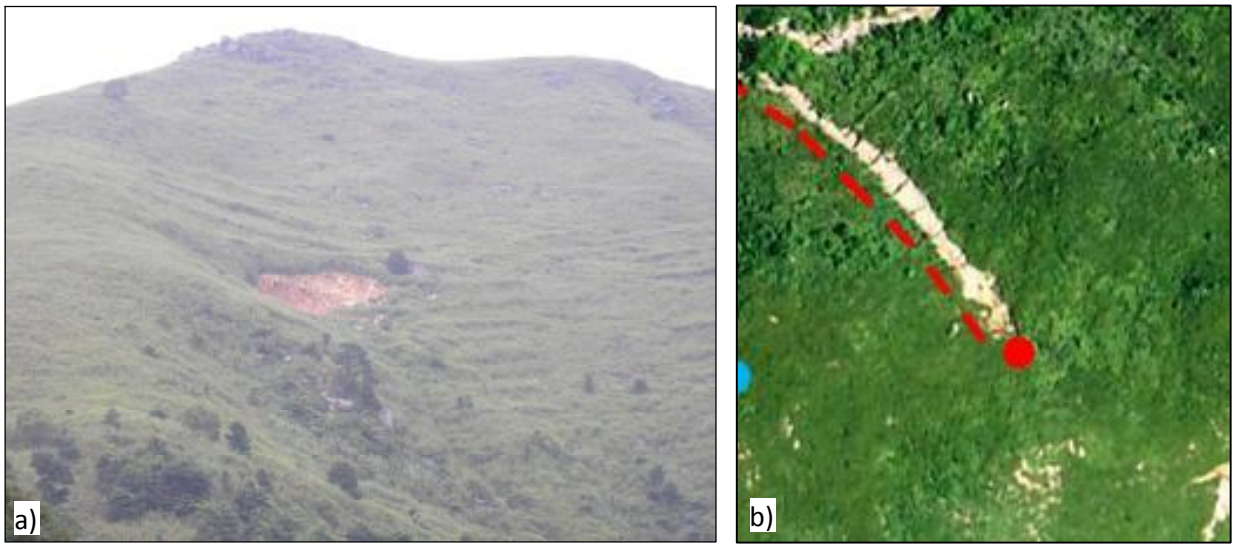

Figure 1: a) Shallow landslide associated with old terraces on northern slopes of Tai Mo Shan; b) Debris flow impacted channel with evidence of old terraces that retained debris and may have reduced run-out velocity

No published estimates of the land area covered by old terraces and associated features are available, however, with the authors' extensive mapping experience in this landscape it is considered that evidence of old terraces are widespread across the green, undeveloped terrain in Hong Kong. Areas where terraces are rarely observed include rock cliff, other areas of exposed bedrock (unweathered to slightly weathered), boulders, exhumed corestones, and/or ground slopes greater than 60º. Since the late 1960s, much of the undeveloped terrain containing terraced hillsides have revegetated following major land use changes, government regulations, and rapid natural growth in a tropical climate (**Figure 2**).

Dense vegetation is common in mountainous, sub-tropical environments such as Hong Kong and presents a considerable obstacle to API and field observations of landscape features, especially micro-topographic landforms. However, the Hong Kong case is unique because of the availability of historical photographs from the 1800s as

well as the early record of aerial photographs that show the undeveloped terrain devoid of dense vegetation and almost no forested canopy. Airborne Laser Swathe Mapping (ALSM) and generation of processed ground return LiDAR data is an approach to overcoming the obstacle of dense vegetation on steep terrain. A territory-wide LiDAR dataset was acquired for Hong Kong in late 2010/early 2011 by the GEO (AAM Pty Ltd., 2012).

Figure 2: Aerial photographs ca. 1963 and 2010 indicating extensive revegetation of Hong Kong hillsides as shown in the Shau Kei Wan study area

The combination of a high-quality photographic record (ground and oblique/vertical aerial), recent LiDAR dataset, and numerous existing landslide studies make Hong Kong a prime location to calibrate an indirect mapping approach to detect old terraces and study their implications for slope stability.

Processed ground return point-cloud LiDAR data were processed into a DEM and a derivative hillshade model was useful for visualisation of old terraces and could be used for remote, direct mapping of old terraces and some associated features. Chase et al (2010) used such a technique on a LiDAR-derived hillshade for mapping ancient Mayan terraces in Belize. However, an indirect mapping technique, such as that proposed, may be more efficient at mapping larger areas (scales smaller than 1:20000). Where quantification of terrace locations is necessary, an indirect technique would reduce precision errors although interpretative, direct mapping may provide more accurate representation of terrace features, especially when combined with API and field work. A topographic position index (TPI) has an emerging application towards indirect mapping of terraces.

A TPI, in general, compares the elevation of one location to the mean elevation of an area and was initially developed for mapping and classifying landforms based on slope position. Each positive index value is related to convex landforms, negative to concave landforms, and zero to (sub) horizontal/vertical landforms. The version of the TPI method used was described by Weiss (2001) although previous workers developed the TPI explicitly (Guisan et al., 1999; Jones et al., 2000). TPI was demonstrated to be a useful metric for landform classification by Tagil & Jenness (2008) by a case study in Turkey and was reviewed in Deng (2007).

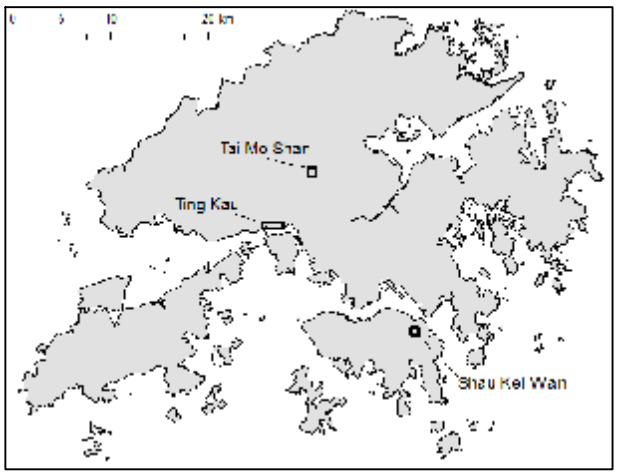

Figure 3: Three case study areas in Hong Kong SAR

Feasibility of the TPI mapping approach to old terraces was investigated for three case study areas with each area having unique landforms, landscape histories, and possibly differing phases or cycles of land usage. The study areas (**Figure 3**) include *Shau Kei Wan* (67 ha) on northeastern Hong Kong Island, *Ting Kau* (141 ha) west of Tsuen Wan, and *Tai Mo Shan* (78 ha) in central New Territories.

METHODS & EQUATIONS

The processed ground return point cloud LiDAR data were interpolated to DEM using the inverse distance weighted (IDW) tool available in the ArcGIS Desktop 10 environment. A variable radius, moving-window defined

by 12 points (default value) and an output cell size of 0.5 m were used as input parameters. A 0.5 m cell size was used because it relates to the specified 0.5 m maximum spacing of points during LiDAR data collection (AAM Pty Ltd., 2012). IDW interpolation is better for reducing precision errors and provides the most accurate and realistic modeling of landforms when compared to other more computationally intensive interpolation methods (Liu et al, 2009; Su & Bork, 2006). Other DEM processing methods could prove useful in the future, however, attempts to use the TIN model for this work were unsuccessful.

Exploration of the TPI technique began with generating a series of TPI surfaces for each case study area. The TPI surfaces were generated using the Land Facet Corridor Designer extension (Jenness et al., 2011) for ArcMap. TPI surfaces were generated from the processed LiDAR DEM using a circular moving-window with the neighbourhood value from 1 m to 5 m at increments of 1 m, and up to 40 m at increments of 5 m (**Figure 4**). Visual comparison of the TPI surfaces and the hillshade model (in which terracing is obvious) indicated that TPI neighbourhood values greater than about 10 m would not detect hillside terraces, and especially not terracettes, so the focus was turned towards the smaller sized neighbourhoods. This is probably due to the fact that the old terraces are usually smaller than about 3 m in rise and run so neighbourhoods that are much larger will be unlikely to detect these relatively small features.

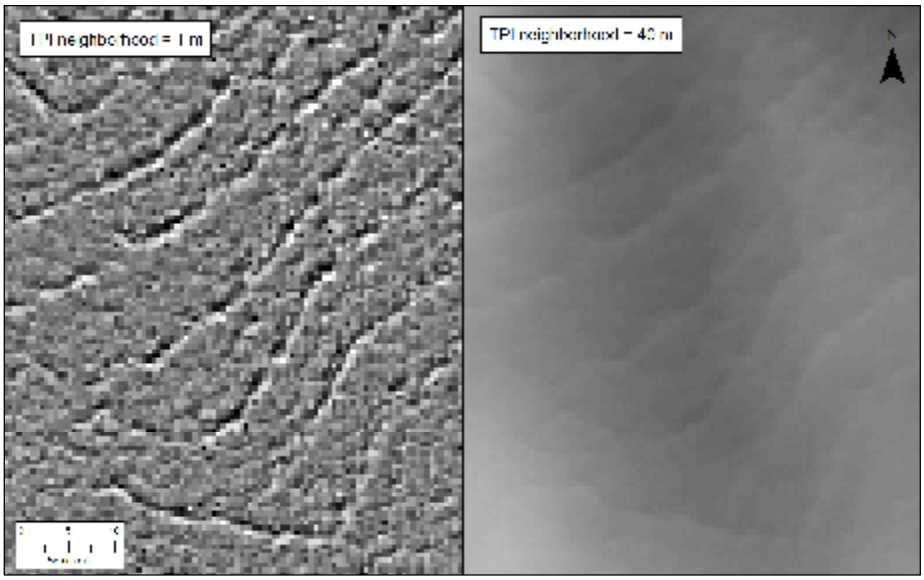

Figure 4: Comparison of TPI neighbourhood size in shrub-grassland vegetated area on Tai Mo Shan

A basic quantitative analysis was performed in order to elucidate the statistical patterns in the distributions of TPI values extracted from each TPI surface. Two to six typical terrace features per study area were identified (total no. of 12 selected terraces) and delineated with a polygon to capture the rise and run of the step-form terrace. Visual identification and delineation of terraces from the TPI surface was aided by the use of orthorectified mosaics of ca. 1963 aerial photographs and the hillshade model. The selected terraces were digitized on-screen, by hand using ArcMap through careful referencing of the various GIS layers (i.e., TPI surface, hillshade model, orthophotos). The TPI values from the selected areas were then extracted from the TPI surface (Tai Mo Shan neighbourhood = 1 m; Ting Kau and Shau Kei Wan neighbourhood = 2 m) and the values were then plotted as frequency distributions in Microsoft Excel (**Figure 5** and **Table 1**).

TPI distributions were generated from 20 bin values determined by the mean and standard deviation of each sample. The number of observations in each sample ranges from 43 to 340 with TPI value ranges from -1.33 to 1.28. The sample size varied according to the size of the selected terrace and TPI values varied depending on the mean and standard deviation of the overall DEM. Direct comparison of TPI values between study areas is problematic since there is a wide range in the topographic relief and plan area amongst the three study areas and "topographic position is an inherently scale-dependent phenomenon" (Weiss, 2001).

Initially, it was hypothesized that the sample distributions would be bimodal (two different modes), since the selected area should correspond to the rise and run of the terrace, which are theoretically orthogonal (i.e., the rise is perpendicular to the run, which is assumed to be horizontal).

In order to test for bimodality in each distribution a bimodality coefficient (b) was calculated from skewness (g_1) and kurtosis (g_2), where

$$b = \frac{g_1^2 + 1}{g_2 + \frac{3(n-1)^2}{(n-2)(n-3)}} \quad (1)$$

The maximum value of b is 1.0 and values of b greater than 0.555 (the value for a uniform population) can indicate bimodality (or multimodality).

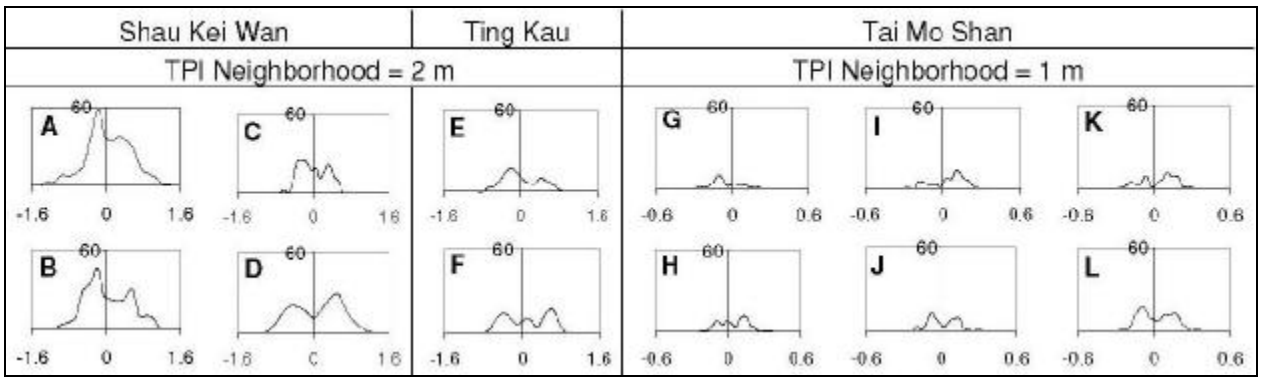

Figure 5: Frequency distributions of TPI values for 12 selected terraces (labels "A" to "L" refer to Table 1)

Study Area	Shau Kei Wan				Ting Kau		Tai Mo Shan					
Label	A	B	C	D	E	F	G	H	I	J	K	L
TPI Neighborhood (m)	2	2	2	2	2	2	1	1	1	1	1	1
n (no. of GRID cells)	340	276	192	190	105	100	43	70	62	68	59	114
MEAN	-0.019	-0.041	-0.029	0.010	-0.056	0.033	-0.073	0.026	0.024	-0.006	0.024	0.002
MEDIAN	-0.052	-0.116	-0.071	0.092	-0.154	0.035	-0.110	0.039	0.058	-0.019	0.063	-0.011
STDEV	0.469	0.456	0.286	0.503	0.365	0.435	0.115	0.118	0.126	0.112	0.126	0.127
MAX	1.279	1.007	0.532	1.126	0.691	0.732	0.176	0.328	0.220	0.288	0.236	0.309
MIN	-1.326	-1.017	-0.628	-1.027	-0.744	-0.724	-0.285	-0.214	-0.284	-0.230	-0.242	-0.263
SKEWNESS (g_1)	-0.040	0.276	0.170	-0.142	0.344	-0.068	0.474	0.041	-0.646	0.132	-0.440	0.100
KURTOSIS (g_2)	-0.032	-0.768	-1.136	-1.056	-0.889	-1.452	-0.330	-0.522	-0.554	-0.662	-0.959	-1.068
BIMOD COEFF (b)	0.334	0.475	0.538	0.512	0.509	0.612	0.423	0.383	0.545	0.411	0.542	0.502

Table 1: Summary statistics for frequency distributions of TPI values for 12 selected terraces (labels "A" to "L" refer to Figure 5)

FIELD INVESTIGATION

Mapping was undertaken by an experienced geomorphologist and engineering geologist for the Ting Kau area in the early stages of this work to determine whether or not the TPI surface reliably produces actual ground conditions. A handheld GPS unit was used in the field to ensure positional accuracy. Two versions of TPI maps were taken into the field, one was a 2D plan and the other was a 2D print of a 3D simulation created in ArcScene. The 2D plan proved difficult for mapping, however the 3D simulation was significantly more useful. Terraces and terracettes that could be mapped with "high confidence" were delineated (**Figure 6**). Most of the field-mapped terraces were rubble-wall type terraces, which are more common in areas of weathered volcanics and bouldery colluvium. Styles & Law (2012) documented evidence of "old stone terrace walls" near a colluvial boulder field in Shau Kei Wan. Where boulders are fewer and rock type more deeply weathered, earthen-step form terraces seem to be more common. However, the type of features is also dependent on the land use practices, types of crop, and the range of ethnicity and heritage of the peoples who constructed them at various times in history. Styles & Law (2012) indicate that Yao hill tribes were likely to have occupied much of the steeper terrain with more recent interaction with the Han from about 900AD and the Hakka from the 1500s. They also state that "well-defined stone

wall oblique-herringbone terraces" nearby and intermixed with "earthen step-form terraces" on Tai Mo Shan (**Figure 7c**) provides evidence of cycles of "different types and/or phases of land usage." In Hong Kong, there is vast opportunity for archaeological and anthropological field and laboratory research along these lines.

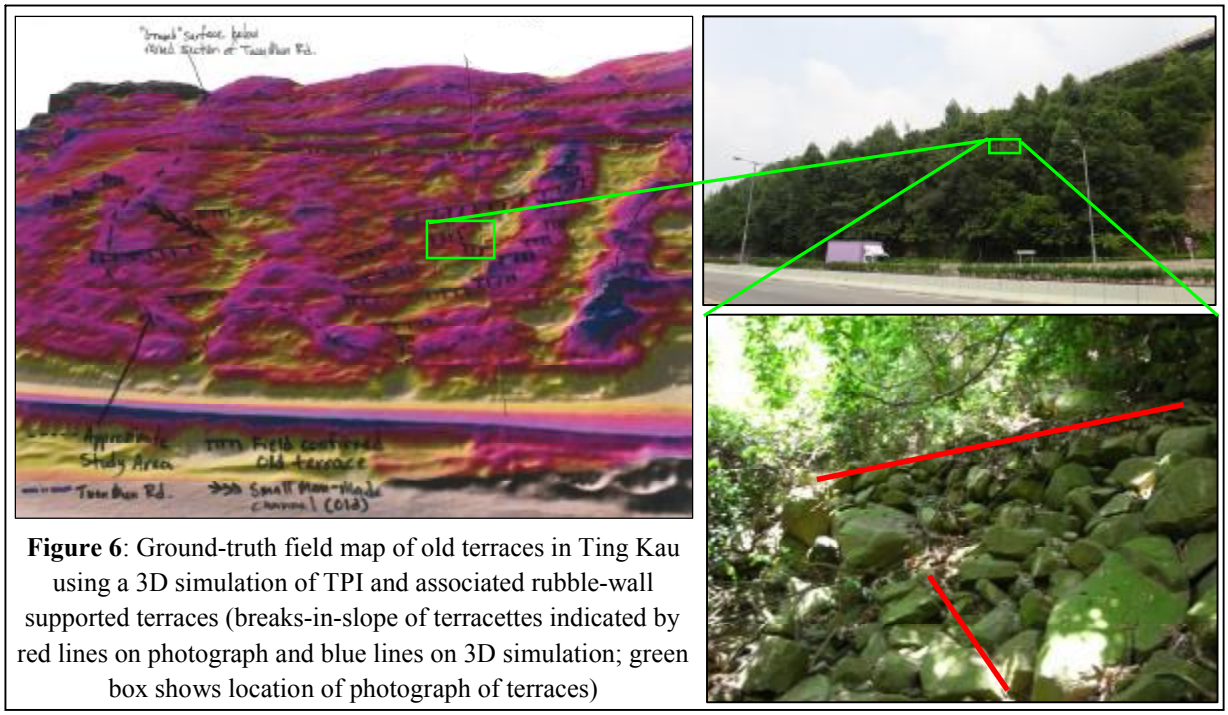

Figure 6: Ground-truth field map of old terraces in Ting Kau using a 3D simulation of TPI and associated rubble-wall supported terraces (breaks-in-slope of terracettes indicated by red lines on photograph and blue lines on 3D simulation; green box shows location of photograph of terraces)

RESULTS

The bimodality coefficients ranged from 0.334 to 0.612 (Table 1), with only one terrace sample fulfilling the bimodality criterion with $b = 0.612 > 0.555$, indicating possible bimodality or multimodality. The remaining 11 samples may belong to a unimodal distribution, although 6 of them have values rather close to 0.555, with values above 0.500 (**Figure 5** and **Table 1**). Although only 12 terraces were selected, the results indicate that the distributions tend towards bimodal ($b > 0.500$) for 58% of the tested samples.

Interpretation of terrace extents, hand digitizing, and IDW interpolation are sources of potential error that have yet to be quantified. These potential errors could affect the outcome of the test for bimodality. Additionally, no effort has yet been made to test the randomness of the sample distributions compared to non-terraced areas or the whole TPI surface (which cover about 70 ha to 140 ha of LiDAR data).

The field validation exercise in Ting Kau was able to document only a few of the terrace features observed from aerial photographs, however far more terraces could be detected when field mapping was aided by use of a TPI surface (**Figure 6**). Dense vegetation is not only a hindrance to API, but also to field mapping. The use of a LiDAR-derived TPI surface in the field enhanced the observers' ability to detect terraces, such that terraces that were normally very difficult to recognize through dense vegetation could be more readily identified and mapped.

DISCUSSION

API of old aerial photographs, performed by skilled specialists, can provide much useful information related to the type, condition, and geometry of the terraces and associated features (**Figure 7a-d**), and in many cases they are clearly evident on the images (**Figure 7a, c**). However, specialist API has limitations related to the quality of the aerial photographs and vegetation coverage. Some of these limitations are overcome with LiDAR, even when vegetation is dense. API is time-consuming, however, with further research and development the TPI could rapidly

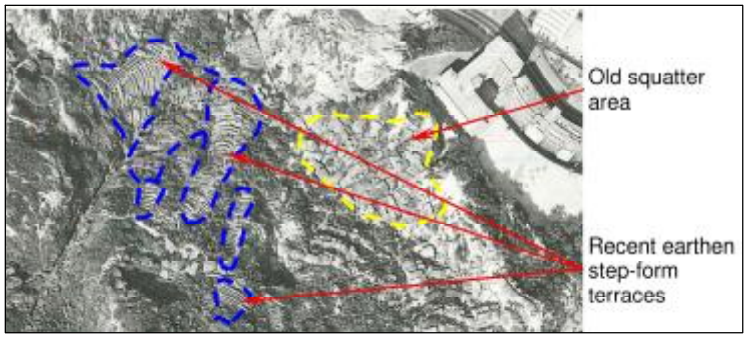

Figure 7a: Recent earthen step-form terraces and squatter platforms in Shau Kei Wan in 1963

map many, or most, of the terraces, and with sufficient computing power, could map the entire territory quickly and efficiently. In Hong Kong, old aerial photographs, especially those acquired in the early 1960s, provide a unique opportunity to benchmark LiDAR interpretation since these photographs reveal the terrain relatively devoid of vegetation (**Figures 2** and **7a-d**).

The hillshade model and API of old aerial photographs have both proved useful, however neither provides a complete, self-contained source of information for mapping terraces. The key limitations from API mapping from old aerial photographs are angle of view (terrain masking), flying height, forward overlap, radial distortion, fortuitous lighting and shadowing. In relation to GIS and indirect mapping, the hillshade model has similar limitations as the TPI; however, since the hillshade provides a "shadow model" of the landscape, the apparent geometry of the terraces can change dramatically depending on the input parameters for Sun angle and direction. This sensitivity to the input parameters means that the interpreted map extents of terraces will not correspond with the actual ground location of the terraces. Essentially, the modeling of shadows in the hillshade will "displace" the actual terrace location (which could be on the order of about 1 m to 10 m). This "apparent displacement" does not occur with the TPI technique because the TPI value is calculated in the same ground location corresponding to the LiDAR-derived DEM (although this location may not correspond to an actual LiDAR ground point since the DEM is interpolated). This is one of the main advantages of the TPI approach compared to other approaches, especially over larger areas.

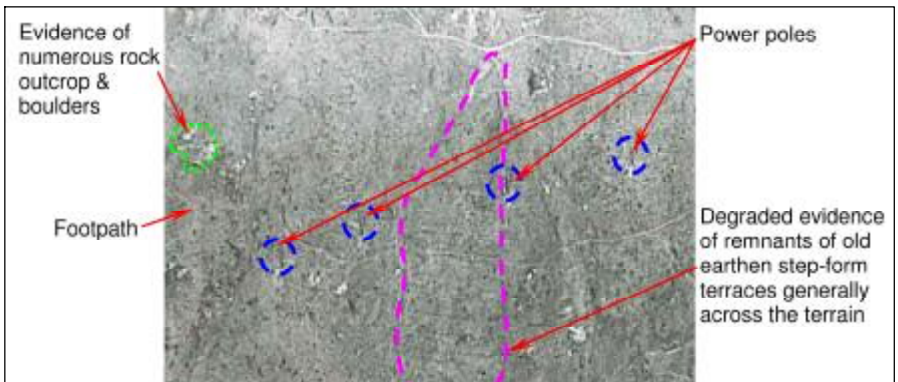

Figure 7b: Less obvious, degraded, earthen step-form terraces in Ting Kau (1963)

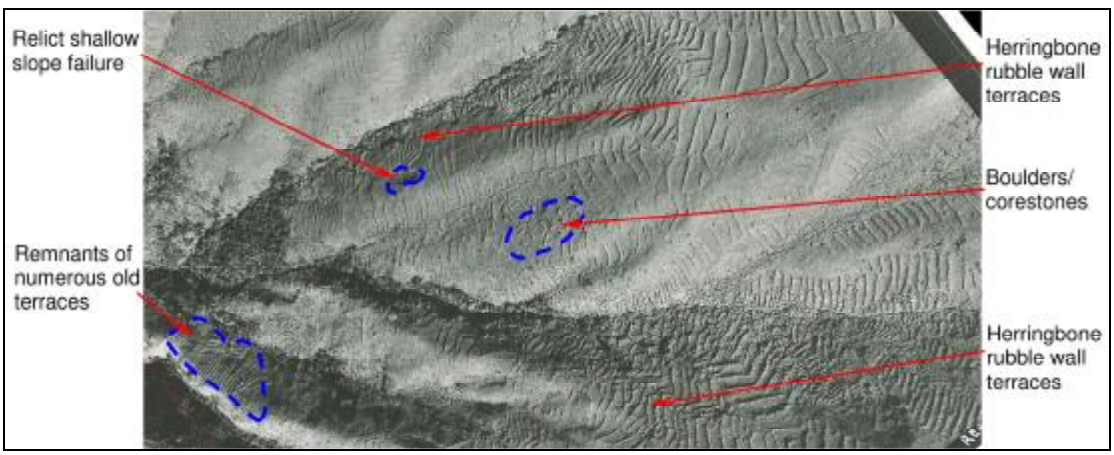

Figure 7c: Specialist API noted hundreds of individual, old terraces of various types across Tai Mo Shan (1963)

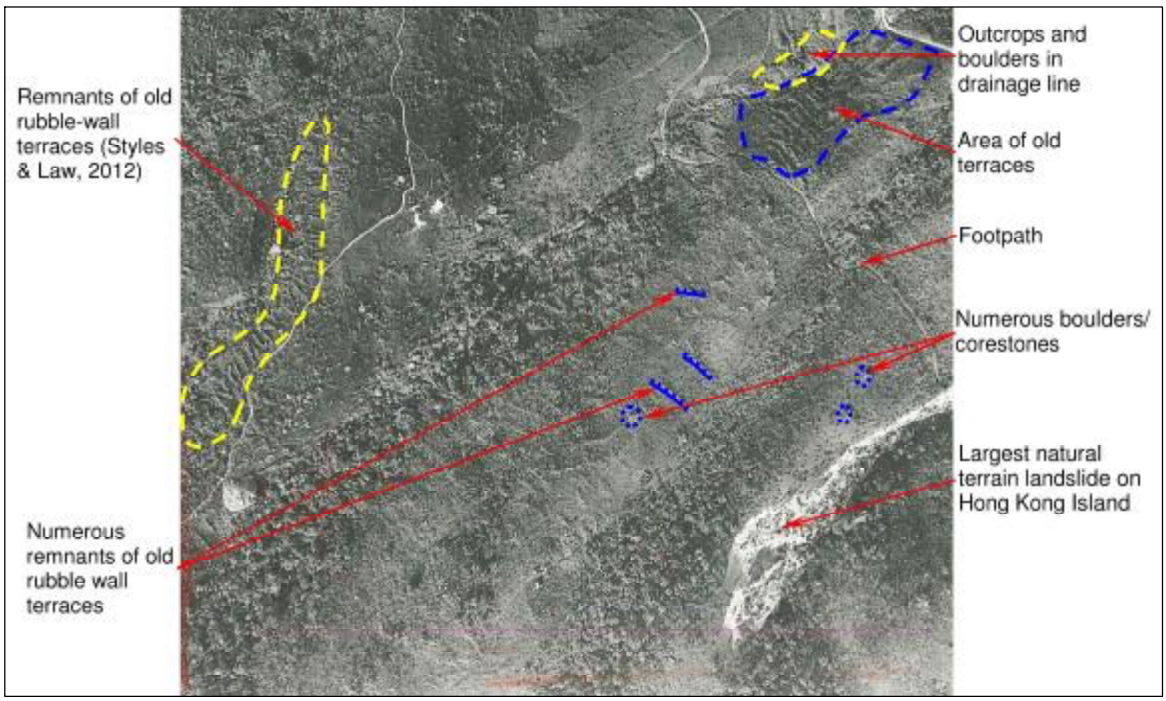

Figure 7d: Remnants of old rubble-wall terraces and a large landslide in Shau Kei Wan (1963)

The high positional accuracy of mapping from LiDAR-derived DEMs is due to high-precision GPS and LiDAR technology. Although modern aerial photography uses similar high-precision GPS technology, radial distortion remains a challenge to API mapping with high positional accuracy. Orthorectification of aerial photographs in a GIS environment may reduce radial distortion, but cannot rectify the images with the same precision as GPS-referencing in the data collection process. Hillshade models generated from LiDAR-derived DEMs are not associated with radial distortion; however there is apparent displacement that varies depending on the modelled orientation of the Sun. These factors indicate that a TPI surface generated from a LiDAR-derived DEM will have the greatest positional accuracy between these three techniques.

The limitations of the TPI approach to mapping terraces is mainly due to the quality and resolution of the LiDAR dataset and the effects of the interpolation technique used to generate a DEM. ALSM from (near) vertically oriented optical sensors is limited in its ability to receive returns from ground surfaces oriented near-vertical. This means that the rise of terrace features is often not returned by vertical ALSM, and therefore these features will mostly be delineated during the DEM interpolation process. This is essentially a lack of data (**Figure 8**), and this can result in over- or under-estimates of terrace extents, especially when combined with the limitations imposed by dense vegetation. And, although the TPI is true to the ground positioning imbued by a LiDAR-derived DEM, the absolute ground extents of terraces will vary when compared to the interpolated DEM. This uncertainty can be reduced by supplementing vertical ALSM with LiDAR collected from oblique, helicopter-borne ALSM, especially when point spacing is very dense.

CONCLUSIONS & FUTURE WORK

An automated approach to detect and map terraces is still in the early phases of research, but the results of the statistical analysis are promising. The hypothesis that the TPI distributions of selected terraces are bimodal has not yet been proven or nullified, nor has an alternate hypothesis been proposed. The initial results indicate that with more careful selection and delineation of terraces and with a more robust analysis of a statistically significant number of samples the quantitative signature of old terraces could be known. Once the TPI values related to

terraces is statistically known, then an algorithm could be developed that relates the statistics to the contiguous linear geometry of TPI values that signify an individual terrace. The vision is that such an algorithm could detect and automatically, indirectly map terraces as polylines or polygons. Such an algorithm would need to be developed in a framework that accounts for the probability of detection and reduces the occurrence of false-positives.

The initial field mapping undertaken in Ting Kau demonstrated the feasibility and reliability of the TPI technique to simulate actual ground conditions. With the use of already available digital field mapping tablets it is anticipated that field validation exercises would be more precise and more efficient.

Once a range of terrace-types can be mapped reliably over large areas then these features can be compared to landslide inventories and detailed morphological maps to develop an understanding of the relationships to landslide susceptibility and slope stability. Landslides that occur recently in the aerial photograph-record are readily mapped since they normally appear as high-reflectance features in otherwise steep, vegetated terrain, and techniques for mapping their geometries are well established. Of course, an automated terrace detection technique would not be able to determine causal relationships. Some important relationships to consider are:

(a) whether or not some landslide geometries are controlled by terraces and associated features,
(b) if the ground disturbance or drainage associated with terraces is a contributing factor to failure, and
(c) if terraces only passively respond to underlying instability that would occur without the terrace-related ground disturbance.

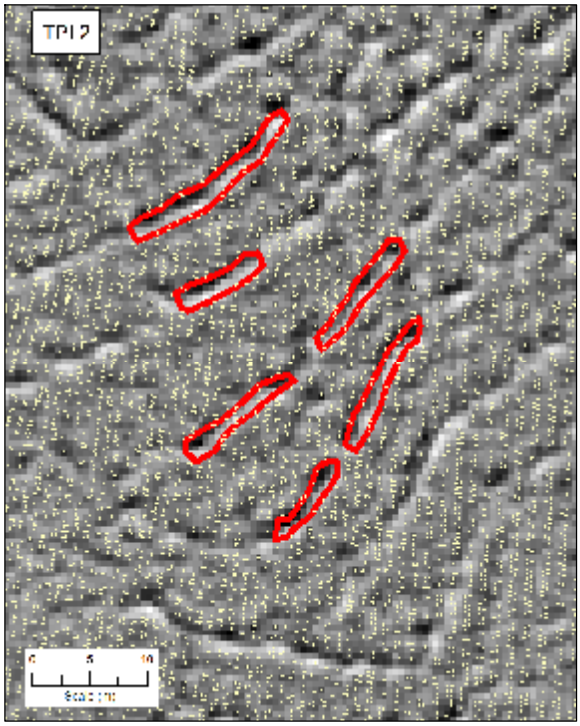

Figure 8: LiDAR ground-return points (yellow) shown to-scale at 20 cm spot-size overlain on TPI surface (selected terraces in red)

A combination of indirect mapping using TPI, specialist vertical and oblique API, and detailed field mapping would improve understanding these important relationships.

ACKNOWLEDGEMENTS

The proprietary LiDAR data were used with agreement of the Civil Engineering and Development Department (CEDD) of the Government of the HKSAR. Acknowledgement is also made to the Director of Lands for use of the aerial photographs. Thanks to Alice Lai and Anthony So of the Geotechnical Engineering Office (GEO/CEDD) for useful discussions, encouragement, advice, and for facilitating use of the data. J. Jenness developed the software for TPI mapping which is freely available at www.jennessent.com. Many thanks to Brandon WU and other colleagues at Fugro (Hong Kong) Ltd. for their assistance and support in this work.

REFERENCES

References from Journals:

Chase, A.F., et al. 2010. Airborne LiDAR, archaeology, and the ancient Maya landscape at Caracol, Belize. Journal of Archaeological Science, p. 1-12.

Deng Y.X. 2007. New trends in digital terrain analysis: Landform definition, representation, and classification. Progress in Physical Geography 31, p. 405-419.

Guisan, A., S. B. Weiss and A. D. Weiss. 1999. GLM versus CCA spatial modeling of plant species distribution. Kluwer Academic Publishers. Plant Ecology, v. 143, p. 107-122.

Heanley, C.M. 1935. Fields of Hong Kong. The Hong Kong Naturalist, Dec. 1935, p. 233-238.

Jones , K.B., D.T. Heggem, T.G. Wade, A.C. Neale, D.W. Ebert, M.S. Nash, M.H. Mehaffey, K.A. Hermann, A.R. Selle, S. Augustine, I.A. Goodman, J. Pedersen, D. Bolgrien, J.M. Viger, D. Chiang, C.J. Lin, Y. Zhong, J. Baker and R.D. Van Remortel. 2000. Assessing Landscape Conditions Relative to Water Resources in the Western United States: A Strategic Approach. Environmental Monitoring and Assessment 64, p. 227 – 245.

Styles, K.A. and Law, M.H. 2012. Some Observations about Man-made Features on Natural Terrain in Hong Kong. The Quarterly Journal of Engineering Geology and Hydrology v.45, The Geological Society, London, p. 131-138.

Su, J. and Bork, E. 2006. Influence of Vegetation, Slope, and LiDAR Sampling Angle on DEM Accuracy. Photogrammetric Engineering & Remote Sensing Vol. 72, No. 11, pp. 1265–1274.

Tagil, S and Jenness, J. 2008. GIS-Based Automated Landform Classification and Topographic, Landcover and Geologic Attributes of Landforms Around the Yazoren Polje, Turkey. Journal of Applied Sciences, 8, p. 910-921.

References from Other Literature:

AAM Pty Ltd. 2012. Territory-Wide Airborne Light Detection and Ranging (LiDAR) Survey. The Government of the Hong Kong Special Administration Region, Civil Engineering and Development Department (Contract No. GE/2008/28), 14 p.

GEO. 2004. Registration and Updating of Records of Features. GEO Circular No. 15. Geotechnical Engineering Office of Hong Kong. 20 p.

Jenness, J., Brost, B, and Beier, P. 2011. Manual: Land Facet Corridor Designer. Available from: http://www.jennessent.com/downloads/Land_Facet_Tools.pdf

Liu, X., Zhang, Z. and J. Peterson. 2009. Evaluation of the performance of DEM interpolation algorithms for LiDAR data. In: Ostendorf, B., Baldock, P., Bruce, D., Burdett, M. and P. Corcoran (eds.), Proceedings of the Surveying & Spatial Sciences Institute Biennial International Conference, Adelaide 2009, Surveying & Spatial Sciences Institute, pp. 771-780. ISBN: 978-0-9581366-8-6.

Ng, K.C., Parry, S., King, J.P., Franks C.A.M., and Shaw, R., 2003. Guidelines for Natural Terrain Hazard Studies. GEO Report No. 138, Geotechnical Engineering Office of Hong Kong. 138 p.

Weiss, A. 2001. Topographic Position and Landforms Analysis. Poster presentation, ESRI User Conference, San Diego, CA. Available, by permission from the author, at http://www.jennessent.com/arcview/TPI_Weiss_poster.htm